
4.1 Electrical Conductivity

Any material can, in principle, be classified as an insulator, semiconductor or metal, frequently based on its electrical resistivity. Insulators have high resistivities ($>10^{10}$ ohm.cm); metals have low resistivities ($<10^{-3}$ ohm.cm); semiconductors have intermediate resistivities. Electrical conduction occurs by the long range migration of either electrons or ions. Migration of ions does not occur to any appreciable extent in most ionic and covalent solids such as oxides and halides. Rather, the atoms tend to be essentially fixed on their lattice sites and can only move via crystal defects. Only at high temperatures, where the defect concentrations become quite large and the atoms have a lot of thermal energy, does the ionic conductivity become appreciable, e.g. the conductivity of NaCl at $\sim 800^\circ\text{C}$, just below its melting point is $\sim 10^{-3}$ S/cm, whereas at room temperature, pure NaCl is an insulator.

The electronic structures of metals, semiconductors and many solids may be described in terms of band theory. The “chemical approach” to band theory is to take molecular orbital theory, as it is usually applied to small, finite-sized molecules and to extend the treatment to infinite, three-dimensional structures. In the molecular orbital theory of diatomic molecules, an atomic orbital from atom 1 overlaps with an atomic orbital on atom 2, resulting in the formation of two molecular orbitals (either σ orbitals or π orbitals) that are delocalized over both atoms. One of the molecular orbitals is “bonding” and has lower energy than that of the atomic orbitals. As the number of molecular orbitals increases, the average energy gap between adjacent molecular orbitals must decrease. (1-2).

The polymer may store charge in two ways. In an oxidation process, it could either lose an electron from one of the bands or it could localize the charge over a small section of the chain.

Localizing the charge causes a local distortion due a change in geometry, which costs the polymer some energy. However, the generation of this local geometry decreases the ionization energy of the polymer chain and increases its electron affinity making it more able to accommodate the newly formed charges. This method increases the energy of the polymer less than it would if the charge was delocalized and, hence, takes place in preference of charge delocalization. According to band theory of solids, the band of energies permitted in a solid is related to the discrete allowed energies, the energy levels of single, isolated atoms. When the atoms are brought together to form a solid, these discrete energy levels become perturbed through quantum mechanical effects, and many electrons in the collection of individual atoms occupy a band of levels in the solid called the valence band. Empty states in each single atom also broaden into a band of levels that is normally empty, called the conduction band. Just as electrons at one energy level in an individual atom may transfer to another empty energy level, so electrons in the solid may transfer from one energy level in a given band to another in the same band or in another band, often crossing an intervening gap of forbidden energies called band gap or forbidden energy gap E_g . In other words, E_g is the energy difference between the valence band (VB) and conduction band (CB) as shown in Figure 4.1

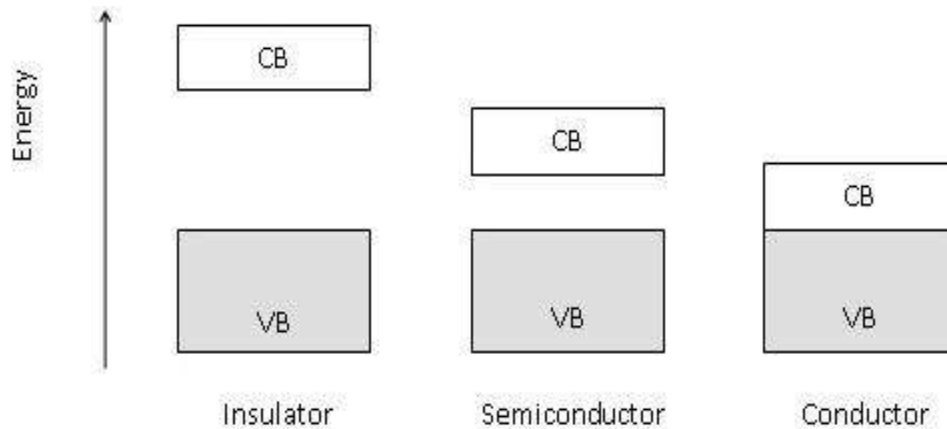


Figure 4.1 : Block diagram of energy band

However, simple band theory is not sufficient to explain the electrical behavior of conducting polymers. For example, simple band theory cannot explain why the charge carriers, usually electrons and holes in polyaniline are spin less. In order to overcome these and other difficulties, the concepts of solitons, polarons and bipolarons have been used since the 1980s to explain the electronic behavior of conducting polymers.

Removal of an electron from the top of the valence band of polyaniline, gives rise to vacancy (radical cation) that is completely delocalized. Only partial delocalization occurs, which extends over some monomeric units leads to a lattice distortion. The energy level associated with this radical cation is placed in the band gap (mid gap level). Following solid-state physics terminology, a partially delocalized radical cation is called polaron. The spin of polaron is $\frac{1}{2}$. If a second electron is removed from the polymer chain, two polarons are obtained, but if the second electron is extracted from a polaron, a bipolaron is created. Low doping levels give rise to polarons, where as higher doping levels produce bipolarons.

A bipolaron is also associated with a lattice distortion. The two positive charges are not independent, and the bipolaron can be thought of as analogous to the Cooper pair in the theory of superconductivity.

In an electric field polarons and bipolarons can move along the polymer chain by rearrangement of double and single bonds. As the doping level increases, the energies of the bipolarons can overlap and narrow bipolaron bands in the band gap can be created. At a high doping level, even if the polymer is highly conducting, no electron spin resonance (ESR) signal is observed, indicating that the charge carriers are spinless. A quite unusual conduction mechanism can be investigated; all bands are either totally filled or empty and mobile bipolarons, instead of electrons, transport the current.

4.1.1 Theory of conduction mechanism

Frames, or lattices consisting of mass points connected by rigid bonds or central-force springs, are important model constructs that have applications in such diverse fields as structural engineering, architecture and materials science. Let us consider a simplest conjugated polymer polyacetylene, where units of CH_2 are linked linearly with alternate double and single bonds with two carbons and two hydrogens. The two Kekulé structures derived from this structure are doubly degenerate energetically. Two energetically equal structures at a point couple to give a surface effect known as Kink or soliton. The term soliton means a solitary wave, implying a non-linear phenomenon involving non-dispersive transport of energy in a dispersive medium. In conjugated systems, solitons may be neutral, positively or negatively charged according to the number of electrons in the π orbital. The difference between the number of bonds and the number of degrees of freedom in these lattices determines the number of their zero-frequency 'floppy'

modes'. When these are balanced, the system is on the verge of mechanical instability and is termed isostatic [3]. It has recently been shown that certain extended isostatic lattices exhibit floppy modes localized at their boundary. These boundary modes are insensitive to local perturbations, and seem to have a topological origin, reminiscent of the protected electronic boundary modes that occur in the quantum Hall effect and in topological insulators. Here, we establish the connection between the topological mechanical modes and the topological band theory of electronic systems, and we predict the existence of new topological bulk mechanical phases with distinct boundary modes.

In charge transport, it is impossible for a soliton to hop from one chain to a nearby chain due to a topological constraint, but this is possible in the case of polarons and bipolarons. Thus polarons and bipolarons are important in three-dimensional charge transport. Variable-range hopping, or Mott variable-range hopping, is a model describing low-temperature conduction in strongly disordered systems with localized charge-carrier states [4-5]. It has a characteristic temperature dependence of

$$\sigma = \sigma_0 e^{-(T_0/T)^{1/4}}$$

for three-dimensional conductance, and in general for d-dimensions

$$\sigma = \sigma_0 e^{-(T_0/T)^{1/(d+1)}}$$

Hopping conduction at low temperatures is of great interest because of the savings the semiconductor industry could achieve if they were able to replace single-crystal devices with glass layers.

Various expressions for temperature dependence of conductivity in different temperature regions are given below

$$\sigma (T) = \exp [-(T_0/T)^{1/4}] \quad \text{at higher temperature}$$

$$\sigma (T) = \exp [-(T_0/T)^{1/2}] \quad \text{at lower temperature}$$

For very low temperatures, the conductivity follows the relation:

$$\sigma (T) = \sigma_0 [-(T/T_0)^{-1/3}]$$

Where, $T_0 = 15.1 K_2 / k_B u_w$ and $\sigma_0 \propto f_2(\infty) u_w^2 / T$

Where u_w is the weight average conjugation length, K_2 is a constant for each polymer depending on the oxidation potential, the reduction potential and band gap of polymer, $f_2(\infty)$ is a interchain hopping frequency per unit volume. The Mott type temperature dependence can also result from the effect of finite conjugation length on the frequency of nearest neighbor interchain hopping. The nearest neighbor hopping process with a distribution of activation energies can give same type of exponential temperature dependence for conductivity as obtained for VRH. The fit parameter T_0 is a function of conjugation length (u_w) and σ_0 is proportional to u_w^2 . The effect of conjugation length on hopping frequency depends upon the effect of conjugation length on ionization potential and electron affinity of the polymer. The value of K_2 lies between 1.5 and 4 eV/electron for known conducting polymers. The value of K_2 does not vary as a function of the doping level [6].

Mott introduced a simplifying assumption that the hopping energy depends inversely on the cube of the hopping distance (in the three-dimensional case). Later it was shown that this

assumption was unnecessary and this proof is followed here. In the original paper, the hopping probability at a given temperature was seen to depend on two parameters, R the spatial separation of the sites and W their energy separation. Apsley and Hughes noted that in a truly amorphous system, these variables are random and independent and so can be combined into a single parameter, the range $\{R\}$ between two sites, which determines the probability of hopping between them.

Mott showed that the probability of hopping between two states of spatial separation R and energy separation W has the form:

$$P \sim \exp \left[-2\alpha R - \frac{W}{kT} \right]$$

where α^{-1} is the attenuation length for a hydrogen-like localized wave-function. This assumes that hopping to a state with a higher energy is the rate limiting process.

The conjugation length is one of the significant factors that determine the temperature dependence of conductivity. The ratio of high temperature to low temperature conductivity increases by decreasing the conjugation length. The doping process can change the effective conjugation length by the introduction of structural or chemical disorder [7]. The electrical anisotropy of unoriented polymer chains is proportional to the square of the average conjugation length and is independent of doping level, temperature and pressure.

In conducting polymer systems, two types of hopping processes are involved. The carriers can hop from one chain to an adjacent one, that is, interchain hopping. The conjugational defects in the chain lead to intra-chain hopping of carrier that moves along the chain. The energy change during hop between conjugated segments is the difference between the ionization potential of

the hopped from chain segment and the electron affinity of hopped chain segment. This energy difference for doped polymers decreases to zero as the conjugation length becomes effectively infinite. Conjugation length depends upon conditions under which the sample is prepared, such as monomer concentration, electrochemical potential etc [8]. At higher monomer concentrations, the possibility of long chain formation is enhanced. Besides, at lower electrochemical potentials, the reaction rate is slow enough so that the number of conjugational defects is smaller.

Percolation theory is closely related to VRH theory and is often mentioned in one breath something that we will also do here in this Essay. The reason is obvious when we take a look at what goes on in the hopping regime. The effective hopping radius, the distance R where the hopping for available energies is still reasonably possible for a certain temperature T , can be calculated, and this thus results in a sphere around the impurity that is effectively conductive. There then exists a critical radius where the spheres marginally touch each other, thereby forming a network of interconnected conductive material spanning the entire sample through which current can marginally percolate, [9] just like water can percolate through the marginally interconnected pores in a ground-coffee-bean powder. For this reason, the names percolation theory and VRH theory are often used.

4.1.2 Experimental Technique

The specific electrical conductivity of a solid σ is defined as the current (amp) flowing through a centimeter cube of the material under unit electrical potential i.e.

$$\sigma = \frac{IL}{AV}$$

where the sample length is L (cm), its area is A (cm²), and potential is V (volts). The experimental set-up used for the measurement of dc conductivity consists of the following components as shown in Figure 4.3.

- A sample holder consisting of sample, electrodes, leads and a means of securely locating the sample.
 - A means for controlling the ambient atmosphere.
 - A heater capable of giving a variable but linear rate of temperature increase over a broad range of temperatures
 - Keithely 6514 electrometer to measure the resistance of the sample under investigation.
-



Figure 4.2: Experimental set-up for DC measurement

DC electrical conductivity is measured using the above mentioned two-probe setup for the following samples:

- 1) Polyaniline
- 2) Polyaniline - Nickel oxide nanocomposites
- 3) Polyaniline - Iron oxide nanocomposites
- 4) Polyaniline - Zinc oxide nanocomposites
- 5) Polyaniline - Zinc Ferrite nanocomposites

The DC conductivity of all the samples is obtained by measuring high resistance through a piece of the material and using the sample dimensions to calculate from the equation.

$$\sigma = (l/RA)S/\text{cm}^{-1}$$

where l (cm) is the sample thickness, A (cm^2) is its area and R (ohm) is the resistance of the material.

4.1.3 Results and Discussions

4.1.3.1 Polyaniline

Figure 4.3 shows the variation of dc conductivity as a function of temperature for Polyaniline. It is observed that the value of dc conductivity increases with temperature. In the temperature range 30 – 100 °C, the conductivity values are almost constant and increases exponentially in the temperature range 100 – 180 °C. in which the polarons possess sufficient energy to hop between various favorable localized states. The conductivity behavior is the characteristic of amorphous materials.

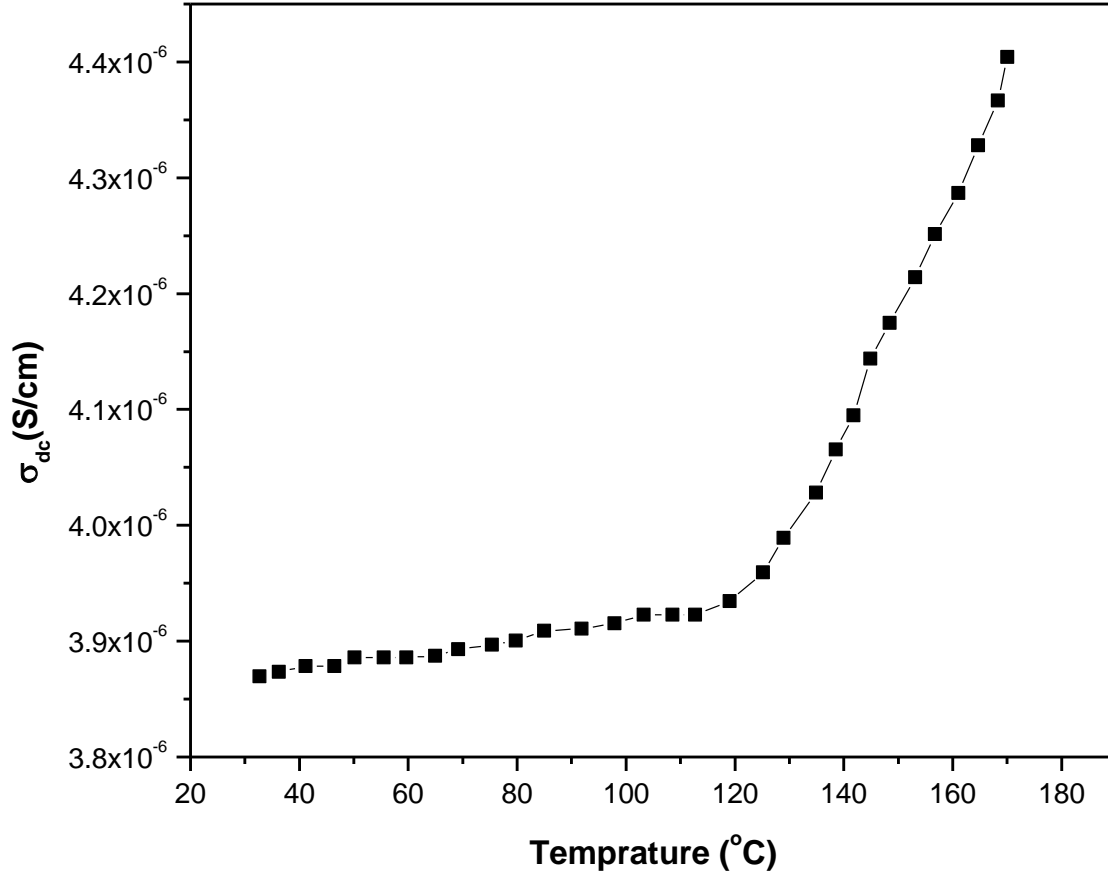


Figure 4.3 shows the variation of σ_{dc} conductivity as a function of temperature for Polyaniline

4.1.3.2 Polyaniline-Nickel Oxide nanocomposites

Figure 4.4 shows the variation of dc conductivity as a function of temperature for Polyaniline-Nickel oxide nanocomposites. It is observed that the value of dc conductivity of these composites increases with increase in temperature. In the temperature range 30 – 120 °C, the conductivity values are almost constant and increase in between temperatures 150 – 180 °C, and a linear increment in the conductivity values are observed. The initial increment in Polyaniline-Nickel oxide nanocomposites may be due to the extended chain length of Polyaniline

in which the polarons possess sufficient energy to hop between various favorable localized states. The conductivity behaviour is the characteristic of amorphous materials. The amorphous polymers can exist in different states depending upon the temperature. At low temperatures, they are hard and glassy materials. At a temperature known as glass transition temperature T_g , they undergo transition to rubber like state. X-ray diffraction pattern and SEM micrograph of Polyaniline-Nickel oxide nanocomposites composites employed in the present investigation show semi-crystalline behavior. Under such conditions, a uniform crystallite is surrounded by amorphous regions. The localized states form extended bandlike structures which may act in trapping the carriers from extended states of crystalline region. Lattice polarization around a charge in localized state may be responsible for multiple phases of conductivity in Polyaniline-Nickel Oxide nanocomposites.

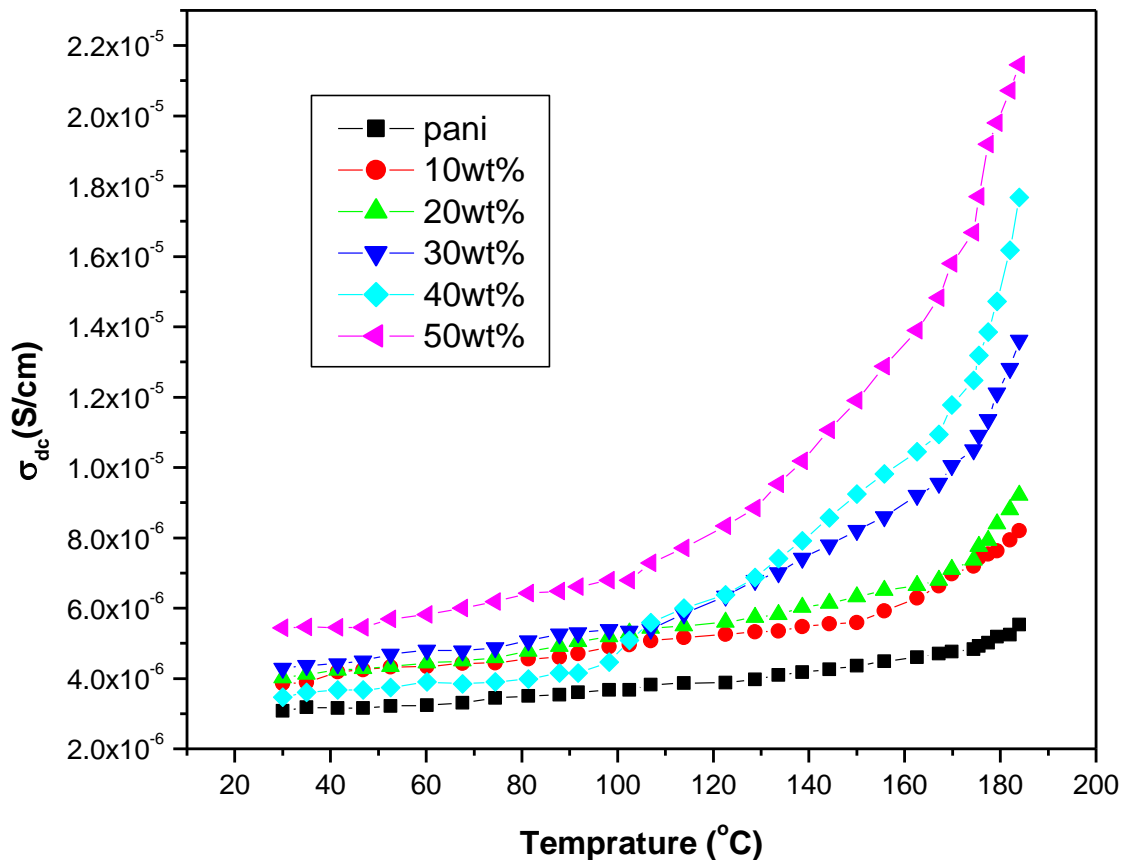


Figure 4.4 : shows the variation of σ_{dc} as a function of temperature for Pani/Nickel Oxide nanocomposites

4.1.3.3 Polyaniline-Iron oxide nanocomposites

Fig 4.5 shows the dc conductivity as a function of temperature and it is observed that the dc conductivity behavior of Polyaniline and Pani/Iron Oxide of different weight percentage are shown in fig 4.5 in the temperature range from 30 to 180 °C. The dc conductivity remains almost constant up to 120 °C and thereafter it increases up to 180 °C, which is the characteristic behavior of semiconducting materials. At higher temperatures conductivity increases because of hopping of ions from one localized state to another localized state. The gradual increase in conductivity is

noticed further which is due to the variation in distribution of Iron oxide particles in Polyaniline .The conductivity varies directly with the temperature, obeying an expression of the following form:

$$\sigma (T) = \sigma_0 \exp [-T_0/T]^{1/4}$$

Where σ is the conductivity, T is the temperature and σ_0 is the conductivity at characteristic temperature T_0 .

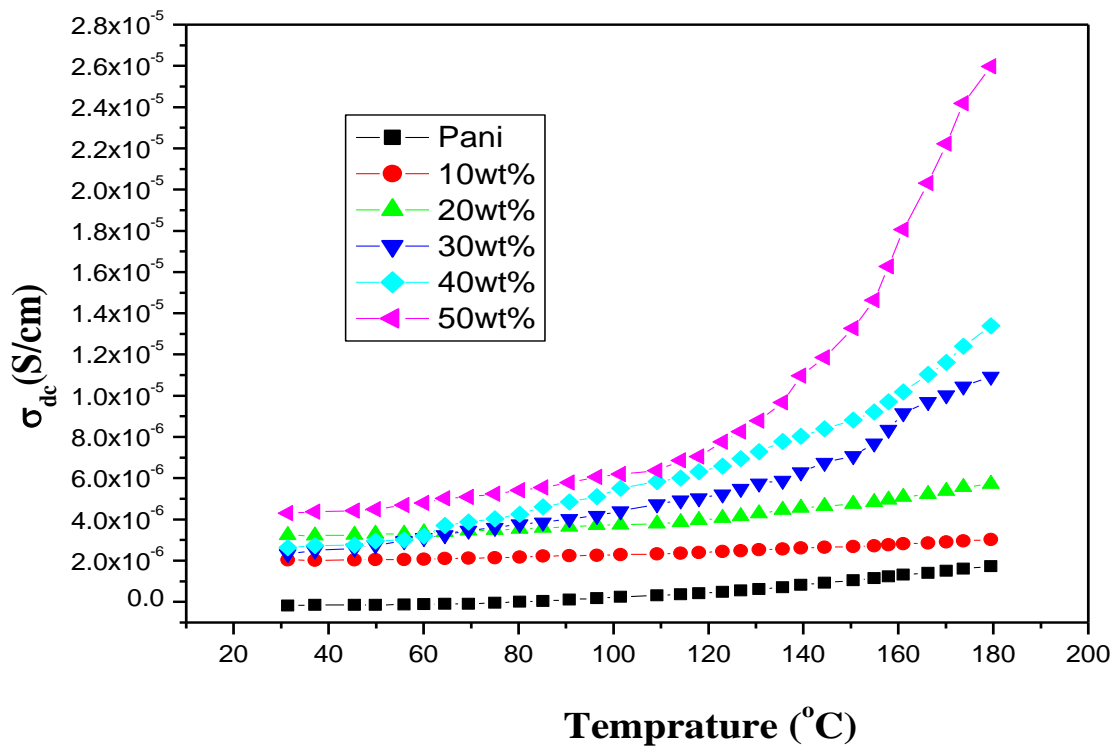


Figure 4.5 : shows the variation of σ_{dc} as a function of temperature for Pani/ Iron Oxide nanocomposites

4.1.3.4 Polyaniline-Zinc Oxide nanocomposites

Figure 4.6 shows the dc conductivity of PANI, PANI /ZnO composites as a function of temperature which varies from 30 to 180°C. The conductivity values are almost constant up to 140°C and there after it increases steadily up to 180°C, which shows the semiconducting material behavior. At higher temperature, conductivity increases because of hopping of charge carriers (polarons) from one localized state to another localized state. Among all the composites, 30wt% shows higher conductivity and it clearly shows that the conductivity is not only the motion of ions (ZnO) but also hopping of charge carriers and also because when PANI mixed with 30wt% ZnO gives more feasibility of matrix's for fast mobility of ions through it easily [10 -13]. The conductivity varies directly with the temperature, obeying an expression of the following form:

$$\sigma(T) = \sigma_0 \exp \left[- \left(\frac{T_0}{T} \right)^{1/4} \right]$$

where: σ is the conductivity, T is the temperature and σ_0 is the conductivity at characteristic temperature T_0 .

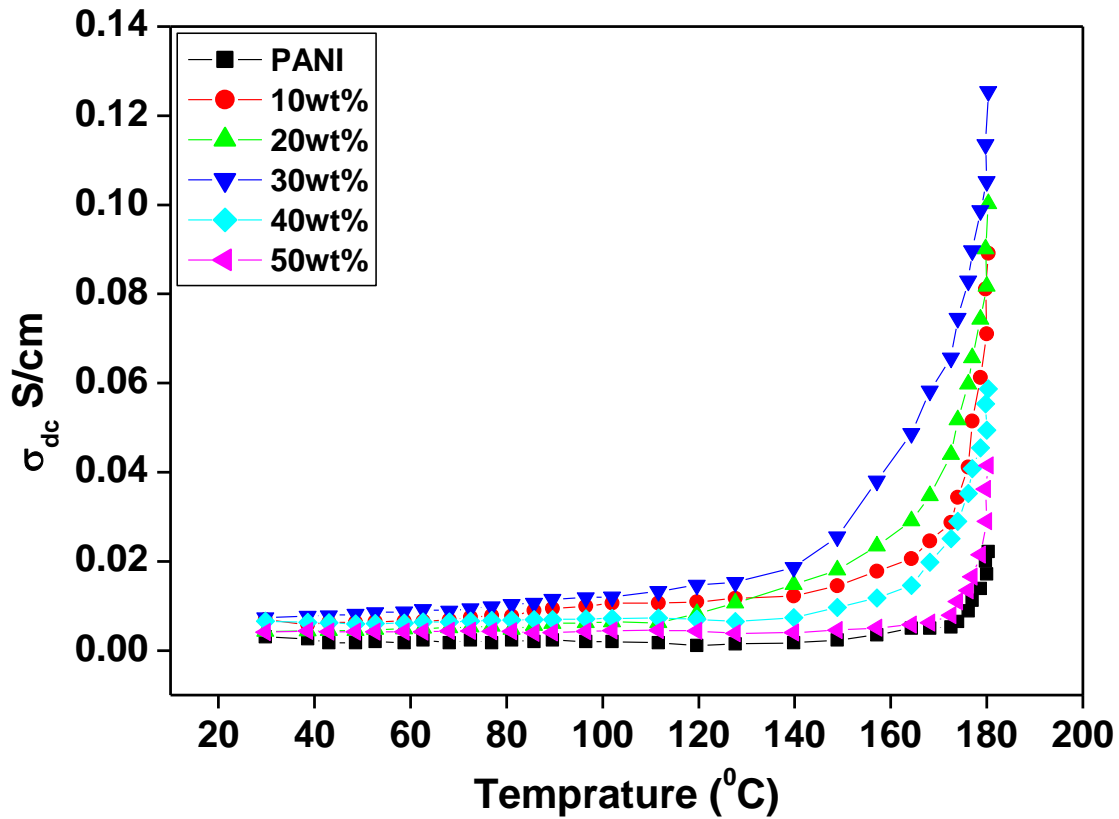


Figure 4.6: shows the variation of σ_{dc} conductivity of Polyaniline/Zno nanocomposites

4.1.3.5 Polyaniline/ Zinc ferrite nanocomposites

Figure 4.7 shows the dc conductivity of Polyaniline and Polyaniline/Zinc ferrite nanocomposites as a function of temperature which varies from 30 to 180 °C. It is observed from the figure, that the dc conductivity remains almost constant up to 130 °C and thereafter it increases steadily up to 180 °C which is the characteristic behavior of semiconducting materials. Among all the nanocomposites, 50wt% shows higher conductivity and it clearly shows that the conductivity is not only the motion of ions of Zinc ferrite but also hopping of charge carriers of polyaniline. The electrical properties in ferrites can be explained on the basis of exchange of electrons between ions of the same element that are present in more than one valence state distributed randomly

over equivalent crystallographic lattice sites (Fe_3+Fe_2+) . It is well known that the change in slope is attributed to the curie temperature or to a change in the conduction mechanism at the Curie temperature and the samples transforms from an ordered ferrimagnetic state to a disordered paramagnetic state with a marked increase in conductivity (14-17).The conductivity varies directly with the temperature, obeying an expression of the following form:

$$\sigma(T) = \sigma_o \exp \left[- \left(\frac{T_o}{T} \right)^{1/4} \right]$$

where σ is the conductivity, T is the temperature and σ_0 is the conductivity at characteristic temperature T_0 .

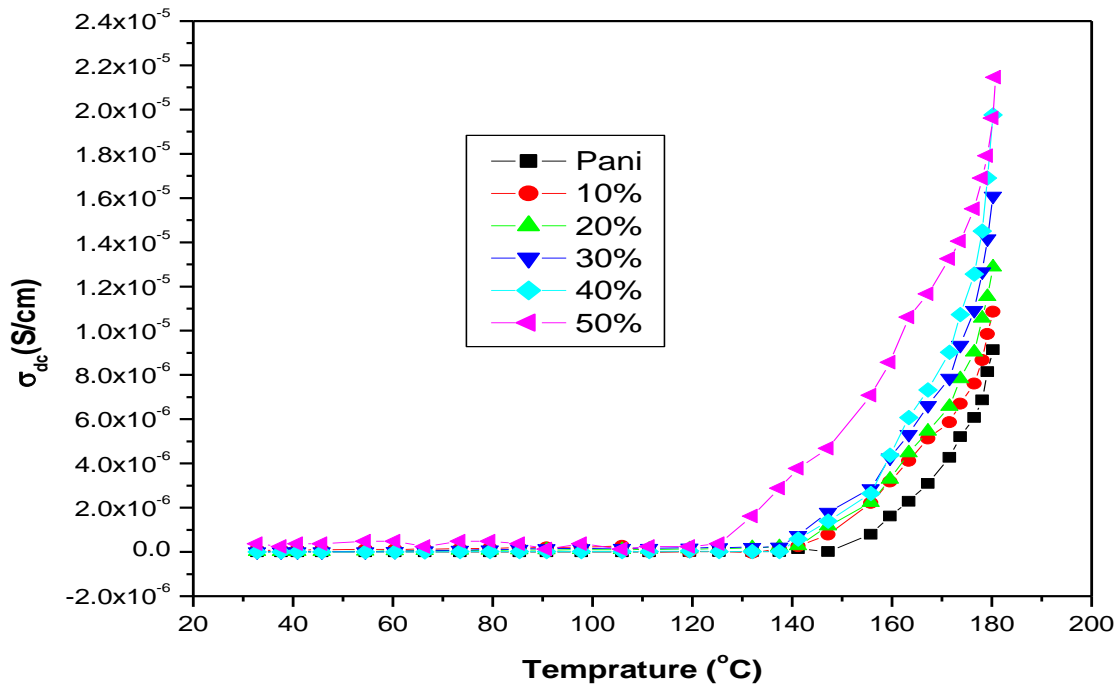


Figure 4.7: shows the variation of σ_{dc} conductivity of polyaniline/Zinc ferrite nanocomposites

4.2 ACConductivity

Electrical conductivity measurements are known to be very sensitive for the study of electronic properties of materials. In amorphous systems dc conductivity measurements are used to study the localization of electronic states, while ac conductivity measurements provide useful information concerning various relaxation phenomenon related to the electrical polarization process. In high frequency measurements, the characteristic hopping lengths and hopping rates of carriers between localized states can be determined. The low frequency data are however, more sensitive to slower relaxation process like the reorientation of dipoles etc. In the latter case most relaxation process can be explained in the Debye theory of energy loss for dipole relaxations [18].

It is well known fact that frequency dependent complex conductivity in case of disordered materials such as polymers can arise from interfacial polarization at contacts, grain boundaries and other inhomogeneities present in the sample [19]. Hence in the following subsection, a brief theoretical approach regarding how the direct current induces polarization effects, in these materials is discussed.

4.2.1 Polarization by Hopping Charge Carriers

Hopping charge carriers which are characterized by the fact that they spend most of the time in localized sites where they are subject only to relatively very small thermal vibrations, but occasionally they make a big jump or hopping transition to some neighboring localized sites which may be one or many atomic spacings away. In strongly disordered solids the normal concept of band conduction by free charge carriers do not apply and instead the carriers become localized and can only move by hopping between localized sites. If these sites form a continuous

connected network the charges may be capable of traversing the entire physical dimensions of the sample and therefore give rise to direct current conduction that would be indistinguishable from free carrier conduction with much lower mobility typically by many orders of magnitude than for the corresponding free band conduction. It is inevitable, however that there exist easier and more difficult hops and that charges execute many reciprocating transitions between pairs of sites linked by easy transitions before making forward jumps to other sites involving more difficult transitions. The probability of a hopping transition may be determined by the combined effect of the distance between the two sites and the potential barrier that has to be overcome the transition may be a thermally assisted hop over the potential barrier or a tunneling transition through the barrier-the latter requiring negligible activation energy. An elementary two site situation is represented in Figure 4.8 in the form of a potential double well separated by an internal barrier and with infinitely high walls outside, indicating negligible probability of escape for the particle. One can assume that the double well accommodates one charge which may occupy either of the two wells, the compensating charge of opposite sign is situated in the neighborhood, possibly between, the two well and is assumed to be rigidly fixed.

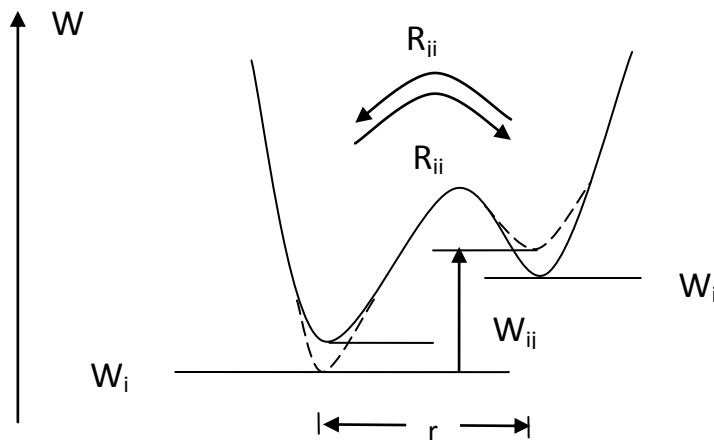


Figure 4.8 Hopping of charge carrier between two potential well

From double well diagram of Figure 4.8. we may define the time-averaged probabilities of occupation in equilibrium, f_i^0 and f_j^0 in terms of the energies W_i^0 and W_j^0 of the two wells.

$$f_i^0 / f_j^0 = \exp (W_{ij}^0/kT) \text{ ----- (1)}$$

Where we have defined $W_{ij} = W_j + W_i$ and the superscripts denotes the equilibrium values in the absence of an externally applied electric field. The condition that the particle with a charge q should certainly be in one of the two wells is

$$f_i + f_j = 1 \text{ -----(2)}$$

Under all conditions, i.e. even in the presence of an electric field. the separation of the energy wells becomes

$$W_{ij} = W_{ij}^0 + qEr \text{ ----- (3)}$$

Where r is the projection of the vector connecting the two wells in space along the direction of the electric field.

This gives rise to a redistribution of the occupation probabilities between the two wells and one can write.

$$f_i = f_i^0 - f ; \quad f_j = f_j^0 + f \text{ -----(4)}$$

And by making the assumption that in the steady state the actual probabilities f_i and f_j are governed by the same Boltzmann law. From equation 1 & 3 with the new energy W given by using $qEr/kT = \delta$, after simple calculation.

$$f^1 = f_i^0 f_j^0 \frac{e - 1}{1 + f_i^0 (e - 1)} = f_i^0 f_j^0 \text{ ----- (5)}$$

The last approximate equality being valid for small values of $q < 1$. In the presence of N identical non-interacting wells the total polarization is given by $P = Nqrf$ which leads to the static susceptibility.

$$\chi_0 = \frac{q^2 \bar{r}^2}{3kT \epsilon_0} \bar{f}_i \bar{f}_j \text{-----} (6)$$

Where the factor 3 in the denominator comes from averaging the projections of the randomly oriented vectors r on the direction of the field and the bar denotes averaging over the factors $f_i f_j$ if these are different for the different wells.

Bearing in mind the fact that qr , may be regarded as the dipole moment of the hopping charge, one can note the similarity of his expression to the dipole orientational polarization given

by equation $\chi(0) = \frac{N\mu^2}{3\epsilon_0 KT}$ this physical difference being that in the latter the dipole changes its

orientation smoothly by free rotation in the medium, while the orientation of the hopping charges is determined by the spatial dispositions of the medium and represent by the potential wells. The distribution of the hopping charges between the allowed sites is influenced by the applied field. It can be noted that the factor $f_i f_j$ would become $1/4$ if all the initial levels were at the same energy.

It is important to note that the transition of a charge q from site i to site j is physically and mathematically indistinguishable from the corresponding of a dipole through the angle. This causes the polarization which leads to observed frequency dependent conductivity.

4.2.2 Theory of AC conductivity in Conductor/Insulator Composites

The ac conductivity of insulator/conductor composites has been modeled by a resistance-capacitance (RC) network, where the conducting dispersants are represented as a resistors and the dielectric of the insulating matrix is represented by capacitors [20, 21]. The complex conductivity σ^* of n parallel components can be expressed by:

$$\sigma^* = \sum \alpha_n \sigma_n^* \quad (\sum \alpha_n = 1) \text{-----(7)}$$

and of n series components by:

$$(\sigma^*)^{-1} = \sum \alpha_n (\alpha_n^*)^{-1} \quad (\sum \alpha_n = 1) \text{----- (8)}$$

where α_n^* and α_n are the complex conductivity and volume fraction of the nth component, respectively. The more general case can be described by [22, 23]:

$$(\sigma^*)^v = \sum \alpha_n (\sigma_n^*)^v \quad (-1 \leq v \leq 1) \text{-----(9)}$$

If $v \rightarrow 0$ then $(\sigma_n^*)^v \rightarrow 1 + v \ln \sigma_n^*$ and equation (9) becomes:

$$\ln \sigma^* = \sum \alpha_n \ln \alpha_n^* \quad \text{----- (10)}$$

Or

$$\sigma^* = \prod (\sigma_n^*)^{\alpha_n} \text{----- (11)}$$

Equation (4) reflects Brown's early suggestion [24] that, $\ln \sigma_n^*$, rather than σ_n^* or $(\sigma_n^*)^{-1}$, should be averaged for a mixture of components.

In a conducting polymer composite having one conducting component, with $\sigma_1^* = \sigma$ for the conducting PANI(where σ is the d.c. conductivity) and $\sigma_n^* = i\omega\epsilon_n$ ($n > 1$, permittivity ϵ_n real, $\omega=2\pi f$, where f is frequency) for the remaining lossless dielectric components of the mixture, equation (11) becomes:

$$\sigma^* = \sigma^{\alpha_1} \prod_{n>1} (i\omega\epsilon_n)^{\alpha_n}$$

i.e. $\sigma^* = \sigma^{\alpha_1} \prod_{n>1} (\epsilon_n)^{\alpha_n} (i\omega)^{1-\alpha_1}$ ----- (12)

Rewriting equation (12) gives:

$$\sigma^* = \beta (i\omega)^\alpha$$
 ----- (13)

where

$$\beta = \sigma^{\alpha_1} \prod_{n>1} (\epsilon_n)^{\alpha_n} \quad (\alpha = 1 - \alpha_1)$$
 ----- (14)

If σ^* is expressed in terms of its real and imaginary components:

$$\sigma^* = \sigma' + i\sigma''$$
 ----- (15)

Then

$$\sigma' = \beta\omega^{-\alpha} \cos(\pi\alpha / 2)$$
 ----- (16)

and

$$\sigma'' = \beta \omega^\alpha \sin(\pi\alpha / 2) \quad \text{-----} \quad (17)$$

The complex conductivity σ^* and the complex permittivity ε^* are related by:

$$\sigma^* = i\omega\varepsilon^* = i\omega(\varepsilon' - i\varepsilon'') \quad \text{-----} \quad (18)$$

Hence, it follows from equation (10) and (11) that:

$$\varepsilon'' = \beta \omega^{\alpha-1} \cos(\pi\alpha / 2) \quad \text{-----} \quad (19)$$

$$\varepsilon' = \beta \omega^{\alpha-1} \sin(\pi\alpha / 2) \quad \text{-----} \quad (20)$$

If only one dielectric material is present, then $n = 2$ and equation (14) becomes:

$$\beta = \sigma(\varepsilon / \sigma)^\alpha \quad \text{-----} \quad (21)$$

where ε_2 and α_2 are now denoted by ε and α for simplification and $\alpha + v = 1$ by definition.

The loss tangent of the composite material is defined by

$$\tan \delta = \varepsilon'' / \varepsilon' \quad \text{-----} \quad (22)$$

Using equations (19) and (20) in conjunction with equation (22), it follows that:

$$\delta = (\pi / 2)(1 - \alpha) = (\pi / 2)v \quad \text{-----} \quad (23)$$

4.2.3 Experimental Technique

The frequency dependent AC conductivity of polyaniline, polyaniline – Nickel oxidenanocomposites, polyaniline–Iron oxidenanocomposites, polyaniline-Zinc oxide nanocomposites and polyaniline – Zinc ferritenanocomposites are studied at room temperature using LCR meter Newton Model PSM-1735. In this experiment, different samples of each composite varying in their weight percentages are investigated for their frequency dependent conductivity. During this course of study, silver electrodes are painted onto the sample surface and then placed under dynamic vacuum during measurement.



Figure 4.9: Experimental set-up for AC conductivity measurement

4.2.4 Results and Discussions

4.2.4.1 Polyaniline

Figure 4.10 shows the variation of ac conductivity as a function of frequency for polyaniline. The conductivity increases with increase in frequency. The ac conductivity exhibits two phases of conductivity where the values are almost constant up to 10^5 Hz and beyond this increases suddenly. Lattice polarization around a charge in localized state may be responsible for multiple phases of conductivity in polyaniline.

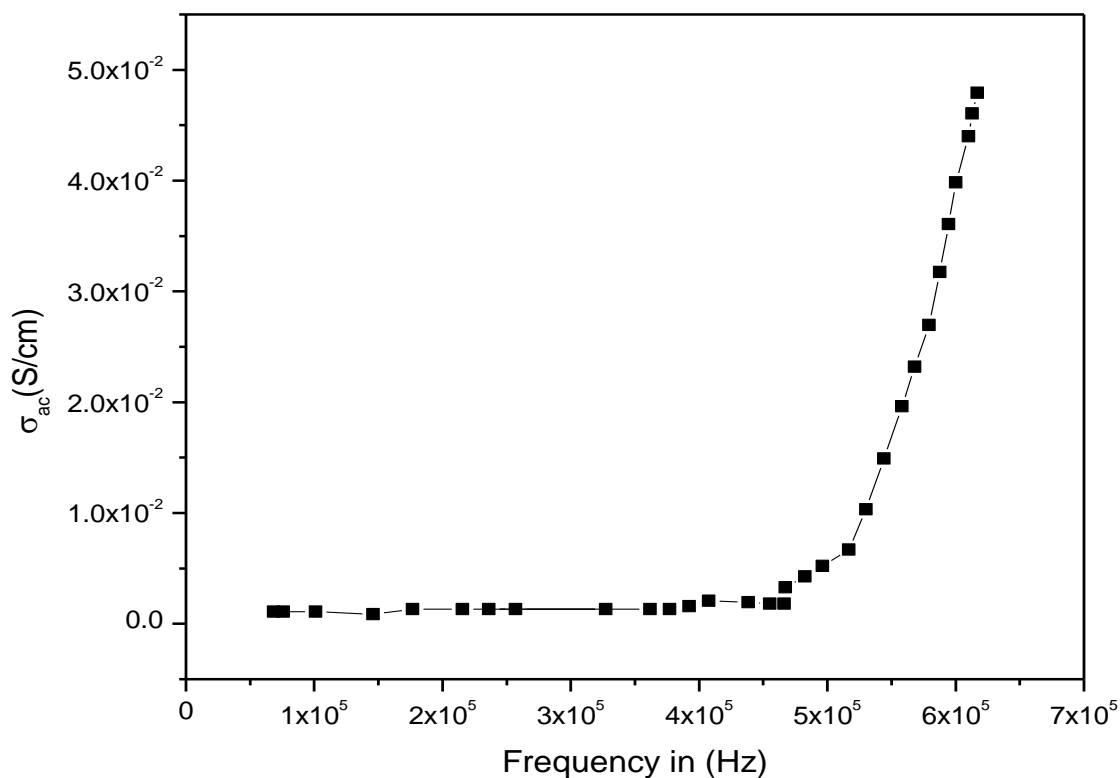


Figure 4.10 shows Variation of σ_{ac} conductivity as a function of frequency for pure Polyaniline

4.2.4.2 PANI and PANI /Nickel oxide nanocomposites

Figure 4.11 shows the variation of ac conductivity as a function of frequency for different wt% of PANI and PANI /Nickel Oxide nanocomposites. It is observed that all the composites show similar behavior which is the characteristic of disordered materials, this is attributed to the variation in distribution of Nickel Oxide particles in the polymer matrix. Lattice polarization around a charge in localized state may be responsible for variation of conductivity in Polyaniline, Pure polyaniline is very light with poor compactness since micro particles are randomly oriented and the linkage among the polymer particles is very weak, resulting in relatively lower conductivity. But, the presence of Nickel Oxide nanoparticles in the composites helps the formation of granular shaped particles, which leads to an increase in the compactness. As the weight percentage of Nickel Oxide in the composites increases, the change in the compactness becomes more significant due to the encapsulation of polymer on the salt. This ultimately leads to an increase in conductivity of the composites.

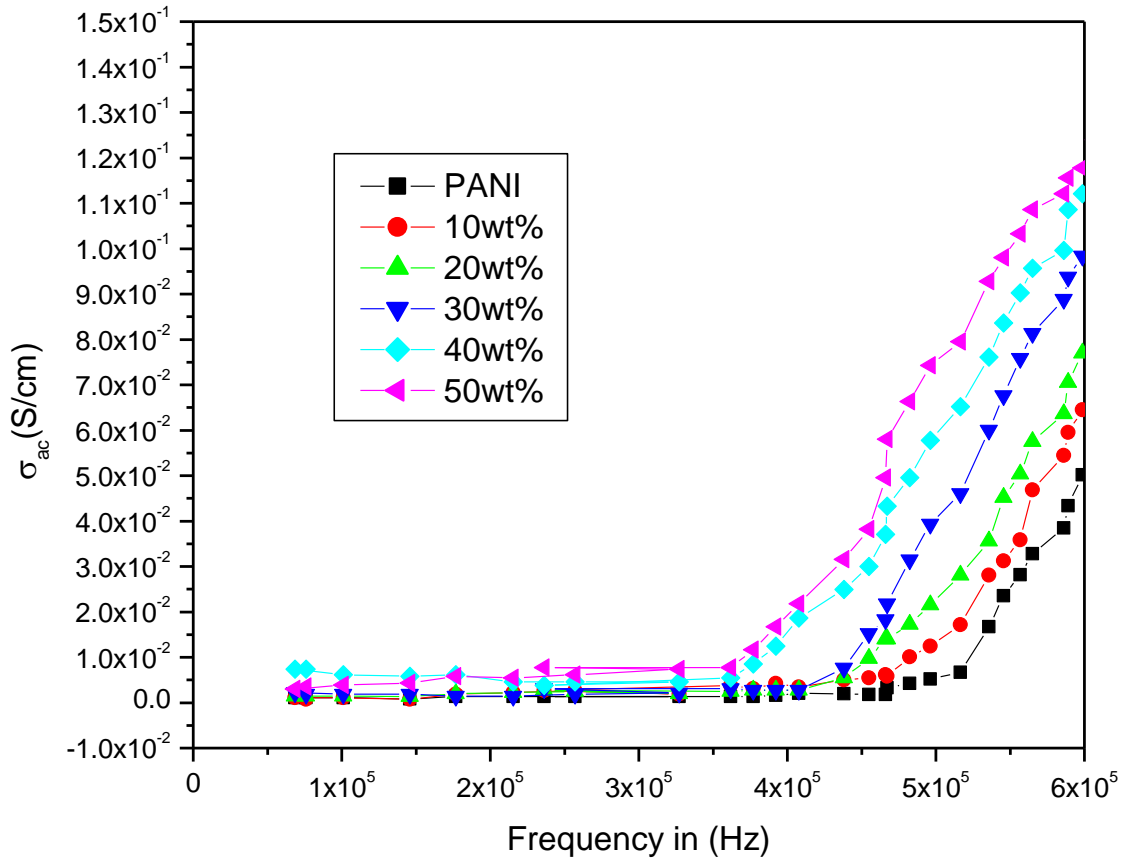


Figure 4.11 shows σ_{ac} conductivity of PANI and PANI /Nickel nanocomposites against applied frequency

4.2.4.3 PANI and PANI /Iron Oxide nanocomposites

Figure.4.12 Shows the variation of ac conductivity as a function of frequency for polyaniline – iron oxide nanocomposites for different wt %. It is observed that in all the cases, σ_{ac} remains constant upto 3×10^5 Hz there after conductivity increases for all the nanocomposites. The anomaly in the conductivity behavior of these composites is due to the variation in the distribution of iron oxide nanoparticles in polyaniline. The increase in conductivity in 50 wt% in polyaniline may be due to the extended chain length of polyaniline which facilitate the polarization of charge carriers

and variation of distribution iron oxide nanoparticles which may support for more number of charge carriers to polarize between favorable localized sites causing increase in conductivity.

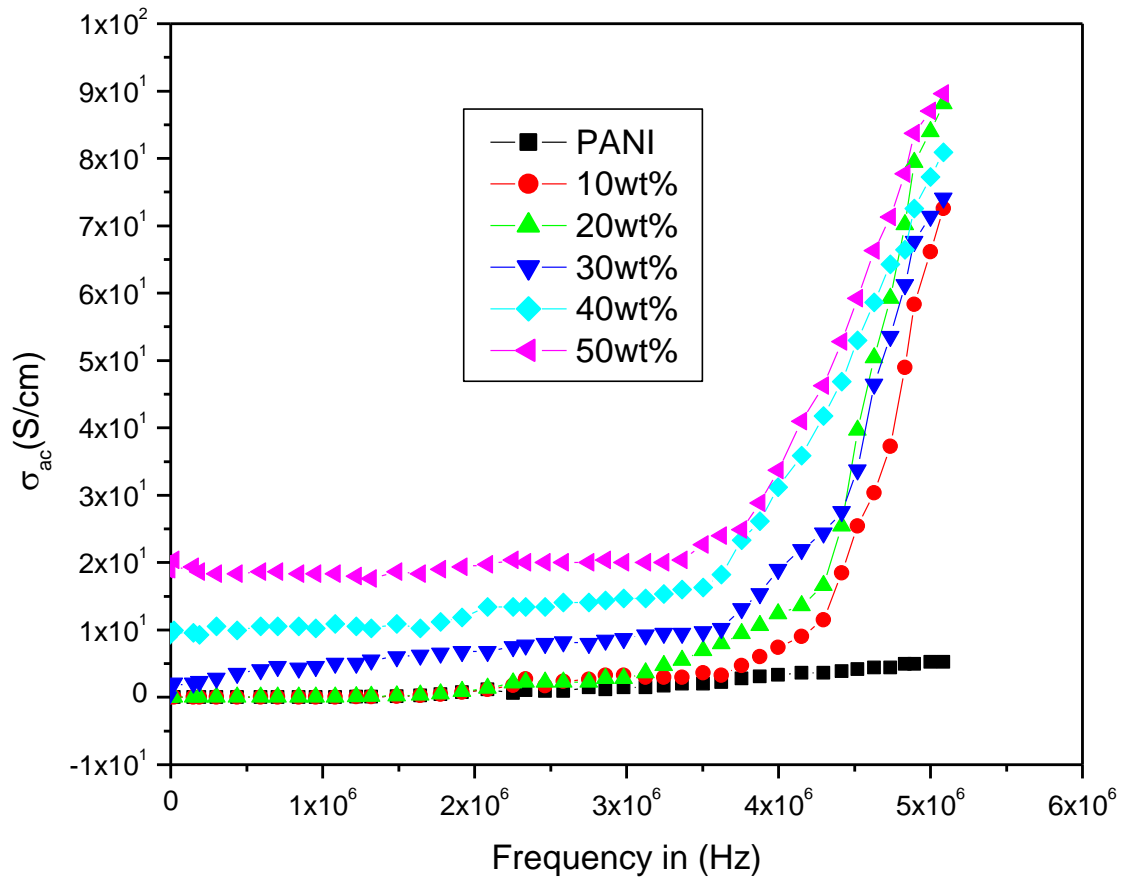


Figure 4.12 shows σ_{ac} conductivity of PANI and PANI /Iron Oxide composites against applied frequency

4.2.4.4 PANI and PANI /ZnO composites

Figure 4.13 shows the ac conductivity of the PANI and PANI /ZnO composites as a function of the frequency at room temperature .It is found that there is increase in the conductivity of the composites for the increase in frequency and this pattern is same for all composites which obeys the universal power law but, at high frequency region, there is an sudden increase in the conductivity with increase in frequency which is the characteristic property of disordered materials. Among all composites, 30wt% shows highest conductivity and this may due to dipole polarization.

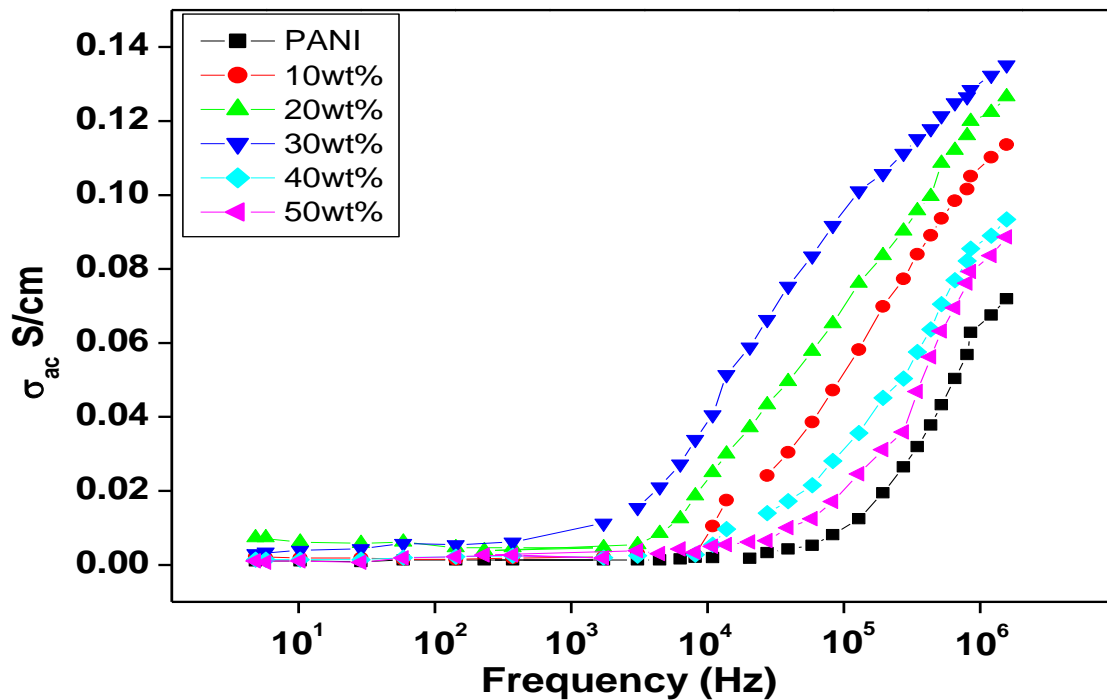


Figure 4.13 shows σ_{ac} conductivity of PANI and PANI /ZnO composites against applied frequency

4.2.4.5 PANI and PANI /Zinc ferrite nanocomposites

Figure 4.14 shows the variation of ac conductivity as a function of frequency with different weight percentages of composites. The conductivity of all the composites increases with increase in applied frequency. It was observed that at lower frequency, the conductivity is almost constant and increased rapidly. It is observed that the magnitude of conductivity of the composites increases with the increase in weight percentage of Zinc ferrite in polyaniline matrix. The stepwise increase in the conductivity shows that these composites follow power law. The conductivity of these composites not only depends on frequency but also on its degree of polymerization, level of protonation, nature of dopants, doping level and crystallinity of the composites. Among all the composites 50 wt% of composite showed the highest conductivity.

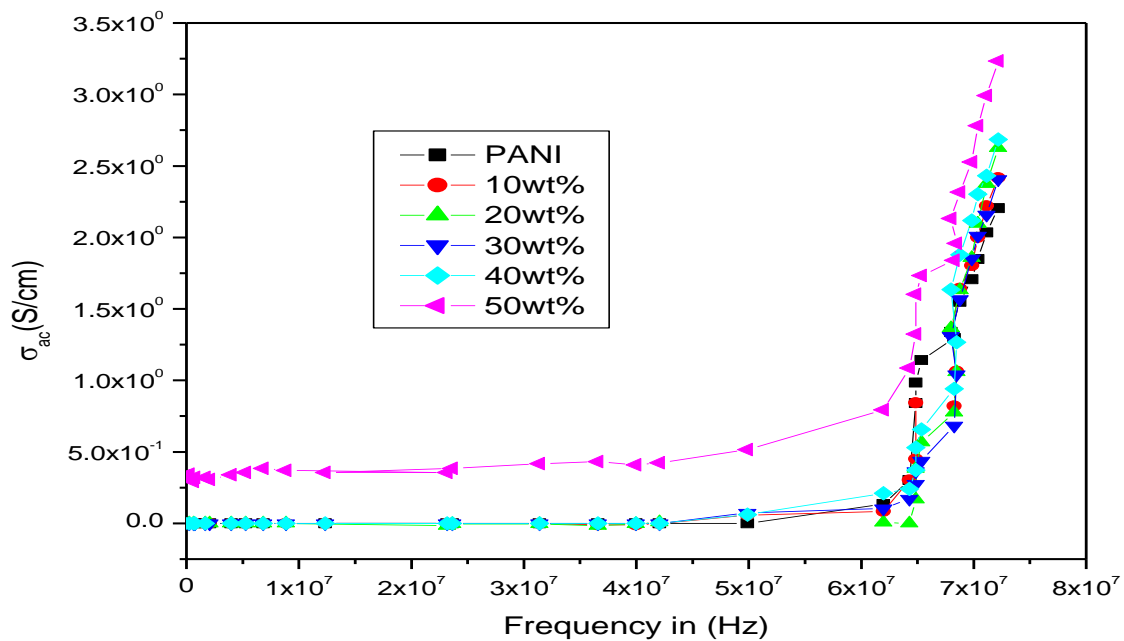


Figure 4.14 shows σ_{ac} conductivity of PANI and PANI /Zinc ferrite nanocomposites against applied frequency

References

-
- (1). A.R. West, *Solid State Chemistry and Its Applications*, John Wiley & Sons Ltd, East Kilbride, Scotland, (1987), 453.
 - (2). D. Jiles, *Introduction to the Electronic Properties of Materials*, Chapman & Hall, London, UK (1994).
 - (3). J. Bernosconi, *Phys Rev. Lett.*, 28 (1972) 1452.
 - (4). A.J. Heeger, S. Kirvelson, J.R. Chreiffer and W.P. Su, *Rev. Mod. Phys.* 60, (1980) 781.
 - (5). D. Emin, *Adv. Phys.*, 24 (1975), 305.
 - (6). P. Sheng, *Phys. Rev. B*, 2,1(1980), 2180.
 - (7). J. Bernosconi, *Phys. Rev. Lett.*, 28, (1972), 1452.
 - (8). R.H. Bughmass and L.W. Shacklette, *Phys. Rev. B*, 29, (1989), 5872.
 - (9). L. Olmedo, I. Chanteloube, A. Germain, M. Petit and E.M. Genies, *Phys. Rev. Lett.*, (1989) 159.
 - (10). T. Dentani., K. Nagasaka., -I.J. Dyes and Pigments, 77, (2008), 59.
 - (11). A. Roy, A. Parveen, R. Deshpande, R. Bhat, A.J. Koppalkar, *Nano part Res*, 15, (2013), 1337
 - (12). X. Zhang, J. Zhu, N.J. Haldolaarachchige., *Polymer*. 53, (2012), 2109.
 - (13). T. Chang, Z. Li, G. Yun, H. Yong Jia., J. Yang. *Nano-Micro Lett*, 5(3), (2013), 163.
 - (14). B.R. Karche, B.V. Khasbardar, A.S. Vaingankar, "Xray, SEM and magnetic properties of Mg-Cd ferrites", *Journal of Magnetism and Magnetic Materials*, vol. 168, (1997), 292.
 - (15). J. M. Song, J.G. Koh, "Studies on the electrical properties of polycrystalline cobalt-substituted lithium ferrites", *Journal of Magnetism and Magnetic Materials*, . 152, (1996), 383.
 - (16). A. A. Sattar, "Temperature Dependence of the Electrical Resistivity and Thermoelectric Power of Rare Earth Substituted Cu – Cd ferrite", *Egypt. J. Sol.* 26, (2003), 113.
 - (17). D. Ravinder, T. S. Rao, "Electrical conductivity and thermoelectric power of lithium-cadmium ferrites", *Crystal Research and Technology*, 25, (1990), 963.
 - (18). J. Bernosconi, *Phys. Rev. Lett.*, 28 (1972) 1452.
 - (19). R.H. Bughmass and L.W. Shacklette, *Phys. Rev. B*, 29 (1989) 5872.
-

(20). L.Olmedo, I.Chanteloube, A.Germain, M.Petit and E.M.Genies, Phys.Rev. Lett.,(1989) 159.

(21) .J.P.Clere, G.Girand, J.M.Laugier and J.M.Lucky, Adv. Phys., 39,(1990) ,191.

(22) .N.F.Mott and E.A.Davis, Elect. Proc. Non-linear Mat., John Wiley publisher . (1987) 325.

(23) .M.Raghu and S.V. Subramanyam, Phys. Rev. B, 43 (1991) 4236.

(24) .J.P.Clere, G.Girand, J.M.Laugier and J.M Lucky, Adv. Phys., 39,(1990) ,191.
